



Role of Plasma and Doping Elements on the Growth and Field Emission Properties of Metallic Carbon Nanotube (CNT) Tip Placed over Cylindrical Surface

Research Article

Suresh C. Sharma*, Aarti Tewari and Ravi Gupta

Department of Applied Physics, Delhi Technological University, Delhi, India

*Corresponding author: suresh321sharma@gmail.com

Abstract. Carbon nanotubes (CNTs) are currently attractive materials for a diverse range of applications because of their extra ordinary mechanical and electrical properties. Their application has already been demonstrated in field emission displays, nanoscale electronic devices, biosensors and hydrogen storage medium. The field emission properties of carbon nanotubes are an important field of study because they give very high values of current density as compared to the already existing field emission devices. The effect of various factors such as plasma parameters, substitutional atoms, dimensional effects, anode-cathode distance etc. on field emission from CNT has also been extensively studied. The present talk will cover the plasma production and effect of doping of hetero-atoms on the growth and field emission properties of Carbon Nanotubes (CNTs) tip placed over a cylindrical surface in complex plasma. A theoretical model incorporating kinetics of plasma species such as electron, ions and neutral atoms including doping elements like nitrogen (N), Boron (B), Potassium (K), Cesium (Cs) and energy balance of CNTs in complex plasma has been developed. The effect of doping elements of N, B, K, and Cs on the growth of CNTs namely the tip radius has been carried out for typical glow discharge plasma parameters. It is found that doping elements affect the radius of CNTs extensively. We obtained small radii for CNT doped with N and large radius for CNT doped with B. The field emission characteristics from CNTs have therefore been suggested on the basis of results obtained. Some of theoretical results are in compliance with the existing experimental observations.

Keywords. Carbon nanotubes; Doping; Field emission; Plasma

PACS. 61.48.De

Received: April 24, 2015

Accepted: November 26, 2015

1. Introduction

Carbon nanotubes (CNTs) show excellent electron field emission properties because of their high aspect ratio, high chemical stability and thermal conductivity. The field emission from CNT is regarded as the most promising application of this nanostructure because they give very high values of current density as compared to the already existing field emission devices. Many extensive studies have been made by many researchers to study the field emission properties of CNTs [1–10]. Doping of CNT is an effective way to tailor the physical and chemical properties of CNTs. However, several groups have studied the field emission properties of doped CNTs [11–17].

Claye *et al.* [11] have achieved reversible insertion of lithium into purified single wall carbon nanotube electrochemically. They showed a continuous decrease in charge transfer resistance upon doping, consistent with the decrease in electronic resistivity of the electrodes. They also showed that the high lithium capacities are not due to double layer capacitance effects but to an actual ion insertion/extraction process in the bulk material.

Zhou *et al.* [12] have studied the p-type doped single wall Carbon nanotube (SWCNT) bulk samples by temperature dependent resistivity and thermo power, optical resistivity and Raman spectroscopy. All these give consistent results for Fermi level downshift (ΔE_F) induced by doping. $\Delta E_F \approx 0.35$ eV and 0.50 eV for concentrated nitric and sulfuric acid doping, respectively. With these values, evolution in Raman spectra can be explained by variation in resonance condition as E_F (Fermi energy level) moves down into the valance band.

Salvato *et al.* [13] have investigated the effect of potassium doping on the transport properties of the aligned single walled carbon nanotube fibers. The temperature dependence of the electrical resistance, current – voltage characteristics and the magneto resistance vs. external magnetic field of the fibers consistently shows that doping enhances the metallic characters of the fibers. In the framework of variable range of hopping theory they suggested that the increase in conduction with potassium doping is due to the increase of density of states.

Wadhawan *et al.* [14] have reported the effects of Cesium (Cs) deposition on the field emission properties of single walled carbon nanotube bundles. Cesium deposition decreases the turn on field for FE (field emission) by a factor of 2.1-2.8 and increases the FE current by six orders of the magnitude.

Xu *et al.* [1] have studied the enhance field emission mechanism by tip-flat emission mode. The results indicate that the radius of apex r is an important factor in field emission with a relationship of field emission factor $\beta \propto r^{-\frac{1}{2}}$, while the tube length has little influence on β .

Levchenko *et al.* [18] have presented the results of hybrid numerical simulation of the growth kinetics of carbon nanowall like nanostructures in the plasma and neutral gas synthesis processes. Low temperature plasma based process was found to have a significant advantage over the purely neutral flux deposition in providing the uniform size distribution of nanostructure. It is shown that nanowall width uniformity is the best in the high density plasmas, worsens in lower density plasmas and is the worst in neutral gas based process.

Keidar *et al.* [19] suggested that length of SWNTs significantly increases (upto 4000 nm),

along with the purity of carbon deposit, when the magnetic field is applied to arc discharge. It is shown that nanotube charge with respect to the plasma as well as nanotube length depend on the plasma density and electric field in the inter electrode gap.

Wang *et al.* [20] have investigated the electron field emission (EFE) characteristics of vertically aligned carbon nanotubes (VACNTs) without and with treatment by the nitrogen plasma. The VACNTs with the plasma treatment showed a significant improvement in the EFE property compared to the untreated VACNTs. It is shown that the significant EFE improvement of the VACNTs after the nitrogen plasma treatment is closely related to the variation of the morphological and structural properties of the VACNTs.

Tewari and Sharma [21] presented the theoretical model to study the growth of carbon nanotube (CNT) on the catalyst substrate surface subjected to the reactive plasma. It is found that the height of the CNT increases with the ion density of the carbon ions and radius of CNT decreases with hydrogen ion density, hence field emission of electrons from the CNT increases.

Bonard *et al.* [2] reported the field emission properties of single-wall carbon nanotube films, with emphasis on current-versus-voltage (I-V) characteristics and current stability. The films are excellent field emitters, yielding current densities higher than 10 mA per cm^2 with operating voltage that are far lower than for other field emitters, but show a degradation of their performance with time.

Wong *et al.* [3] prepared the Silicon Carbide (SiC) nanowires on the silicon substrate using hot filament assisted chemical vapor deposition with solid silicon and carbon source. The silicon nanowire show good field emitting properties as revealed by the current-voltage characteristics.

Bonard *et al.* [4] have studied the emission behavior of single-wall, closed and opened arc discharge multiwall, and catalytically grown multiwall nanotubes, as single emitters and in film form. They suggested that to obtain good performances as well as long emitters lifetimes, the nanotube should be multi-walled and have closed, well-ordered tips.

Kenneth *et al.* [5] demonstrated that an individual nanotube exhibits current saturations above 100 nA of emission current and showed that this current saturation is a direct result of an adsorbate enhanced field emission mechanism. Current saturation results from the displacement of adsorbates from configurations of tunneling enhancement as electric field and current are increased.

Srivastava *et al.* [6] have shown the randomly oriented short and low density carbon nanotubes (CNTs) on silicon substrate. These films have superior emission characteristics compared to high density vertically aligned or randomly oriented bamboo shaped CNTs (BS-CNTs) films. These films were highly crystalline and had many open edges on the outer surface, particularly near the joints of the compartments.

In this paper, we have seen the role of different doping elements on the growth and field emission properties of a carbon nanotube (CNT) tip placed over cylindrical surface. A theoretical model is developed for spherical CNT tip placed over cylindrical surface, which is based on the charge neutrality of the CNT tip, kinetics of various species (electrons, positively charged ions, neutral atoms, and doping atoms) in plasma, number density of the CNT tip and the energy balance of various plasma species and CNT tip.

2. Model

Following the elegant models of the Sodha *et al.* [22, 23] and Tewari and Sharma [24], we consider the plasma containing electrons, positively charged ions and neutral atoms of three different types (1, 2 and 3) and CNT with spherical tip placed over cylindrical surface. We assume singly ionized positive charged ions. Atom 1 refers to the Carbon atom, 2 refers to the Neon, and 3 refers to the doped atoms i.e. Nitrogen (N), Boron (B), Potassium (K) and Cesium (Cs). The initial radius a_0 of the carbon nanotube (CNT) can be estimated by equating the accretion of electrons and positively charged ions on the CNT.

$$\begin{aligned}
 & 4\pi a_0^2 n_e \left(\frac{T_e}{m_e}\right)^{\frac{1}{2}} \exp\left(\frac{-e^2}{a_0 k_B T_e}\right) + 2\pi a_0 h_0 n_e \left(\frac{T_e}{m_e}\right)^{\frac{1}{2}} \exp\left(\frac{eV_s}{k_B T_e}\right) \\
 &= \pi a_0^2 \left(1 + \frac{e^2}{a_0 k_B T_e}\right) \left[n_{i1} \left(\frac{T_{i1}}{m_{i1}}\right)^{\frac{1}{2}} + n_{i2} \left(\frac{T_{i2}}{m_{i2}}\right)^{\frac{1}{2}} + n_{i3} \left(\frac{T_{i3}}{m_{i3}}\right)^{\frac{1}{2}} \right] \\
 & \quad + \left[n_{i1} \left(\frac{T_{i1}}{m_{i1}}\right)^{\frac{1}{2}} + n_{i2} \left(\frac{T_{i2}}{m_{i2}}\right)^{\frac{1}{2}} + n_{i3} \left(\frac{T_{i3}}{m_{i3}}\right)^{\frac{1}{2}} \right] \\
 & \quad \times \left[\frac{2}{\sqrt{\pi}} \left(\frac{eV_s}{k_B T_i}\right) + \exp\left(\frac{eV_s}{k_B T_i}\right) \operatorname{erfc}\left(\frac{eV_s}{k_B T_i}\right)^{\frac{1}{2}} \right],
 \end{aligned}$$

where

h_0 = height of the CNT,

V_s = surface potential on the cylindrical surface,

n_e = number density of electrons,

T_e = electron temperature,

k_B = Boltzmann's constant,

T_i = ion temperature,

n_{i1} = number density of ions of type 1,

m_{i1} = mass of ions of type 1,

n_{i2} = number density of ions of type 2,

m_{i2} = mass of ions of type 2,

n_{i3} = number density of ions of type 3,

m_{i3} = mass of ions of type 3,

e = electronic charge

Charge neutrality equation

$$Q n_{cnt} + n_{i1} + n_{i2} + n_{i3} = n_e, \quad (2.1)$$

where Q = charge on CNT, n_{cnt} = number density of CNT.

Charging of the CNT

The charge is developed on the CNT due to accretion of electrons and positively charged ions on the surface of the CNT, which is given by the equation:

$$\frac{dQ}{d\tau} = I_{i1cnt} + I_{i1cntcyl} + I_{i2cnt} + I_{i2cntcyl} + I_{i3cnt} + I_{i3cntcyl} - \gamma_e (I_{ecnt} + I_{ecntcyl}), \quad (2.2)$$

where $I_{ecnt} = \pi a^2 \left(\frac{8k_B T_e}{\pi m_e} \right)^{\frac{1}{2}} n_e \exp[Q\alpha_e]$, is the electron collection current at the surface of spherical CNT tip and $\alpha_e = \left(\frac{e^2}{ak_B T_e} \right)$, $I_{ijcnt} = \pi a^2 \left(\frac{8k_B T_i}{\pi m_j} \right)^{\frac{1}{2}} n_{ij} [1 - Q\alpha_i]$, is the ion collection current due to the j^{th} atom (1, 2 or 3) at the surface of spherical CNT tip.

$I_{ecntcyl} = \pi a h \left(\frac{2\pi k_B T_e}{m_e} \right)^{\frac{1}{2}} n_e \exp \left[\frac{eV_s}{k_B T_e} \right]$, is the electron collection current at the cylindrical surface of CNT.

$I_{ijcntcyl} = n_{ij} a h \left(\frac{2\pi k_B T_i}{m_j} \right)^{\frac{1}{2}} \left(\frac{2}{\sqrt{\pi}} \left(\frac{eV_s}{k_B T_e} \right)^{\frac{1}{2}} + \exp \left[\frac{eV_s}{k_B T_e} \right] \operatorname{erfc} \left[\left(\frac{eV_s}{k_B T_e} \right)^{\frac{1}{2}} \right] \right)$, is the ion collection current due to j^{th} type of atom (1, 2 or 3) at the cylindrical surface of CNT, $\alpha_i = \left(\frac{e^2}{ak_B T_i} \right)$, where a is the radius of the spherical tip of the CNT placed over cylindrical surface (i.e. radius at any instant of time), γ_e is the sticking coefficient of the constituent electron at the surface of the spherical CNT tip.

Growth rate equation of electrons

$$\frac{dn_e}{d\tau} = (\beta_1 n_1 + \beta_2 n_2 + \beta_3 n_3) - (\alpha_1 n_e n_{i1} + \alpha_2 n_e n_{i2} + \alpha_3 n_e n_{i3}) - \gamma_e n_{cnt} (I_{ecnt} + I_{ecntcyl}), \quad (2.3)$$

where β is the coefficient of ionization of the constituent neutral atoms i.e. atom 1, 2 or 3, $\alpha_j(T_e) = \alpha_{j0} \left(\frac{300}{T_e} \right)^k \text{ cm}^3/\text{sec}$, is the coefficient of recombination of electrons and positively charged ions due to j^{th} atom i.e. atom 1 or 2 or atom 3.

First term on the RHS in this equation describes the rate of gain in electron density per unit time due to ionization of neutral atoms, second term describes the decaying rate of electron density due to electron-ion recombination, and third term describes the electron current at the surface of CNT.

Growth rate equation of positively charged ions

$$\frac{dn_{i1}}{d\tau} = \beta_1 n_1 - \alpha_1 n_e n_{i1} - n_{cnt} (I_{i1cnt} + I_{i1cntcyl}), \quad (2.4)$$

$$\frac{dn_{i2}}{d\tau} = \beta_2 n_2 - \alpha_2 n_e n_{i2} - n_{cnt} (I_{i2cnt} + I_{i2cntcyl}), \quad (2.5)$$

$$\frac{dn_{i3}}{d\tau} = \beta_3 n_3 - \alpha_3 n_e n_{i3} - n_{cnt} (I_{i3cnt} + I_{i3cntcyl}), \quad (2.6)$$

First terms on the RHS describes the gain in ion density per unit time due to ionization of neutral atoms, second term describes the electron-ion recombination and third term describes the ion collection current to the surface of CNT.

Growth rate equation of neutral atoms:

$$\frac{dn_1}{d\tau} = \alpha_1 n_e n_{i1} - \beta_1 n_1 + n_{cnt} (1 - \gamma_{i1}) (I_{i1cnt} + I_{i1cntcyl}) - n_{cnt} \gamma_1 (I_{1cnt} + I_{1cntcyl}), \quad (2.7)$$

$$\frac{dn_2}{d\tau} = \alpha_2 n_e n_{i2} - \beta_2 n_2 + n_{cnt} (I_{12cnt} + I_{i2cntcyl}), \quad (2.8)$$

$$\frac{dn_3}{d\tau} = \alpha_3 n_e n_{i3} - \beta_3 n_3 + n_{cnt} (1 - \gamma_{i3}) (I_{i3cntcyl} + I_{i3cntcyl}) - n_{cnt} \gamma_3 (I_{3cnt} + I_{3cntcyl}), \quad (2.9)$$

where $I_{jcnt} = \pi a^2 \left(\frac{8k_B T_n}{\pi m_j} \right)^{\frac{1}{2}} n_j$, is the collection current due to j^{th} type (1, 2 or 3) neutral atoms at the surface of spherical tip CNT, $I_{jcntcyl} = \pi a h \left(\frac{2k_B T_n}{m_j} \right)^{\frac{1}{2}} n_j$, is the collection current due to j^{th} (1, 2 or 3) neutral atom at the cylindrical surface of CNT.

First term on the RHS describes the gain in neutral atom density per unit time due to electron-ion recombination, second term shows the decrement in neutral atom density due to ionization, third term describes the gain in neutral atom density due to neutralization of the atom collected at the surface of CNT, and the last term describes the accretion of neutral atoms of species 1 and 3 on CNT.

Growth rate equation for the mass of CNT

$$\begin{aligned} \frac{dm_{cnt}}{d\tau} = & m_1 \gamma_1 (I_{1cnt} + I_{1cntcyl}) + m_{i1} \gamma_{i1} (I_{i1cnt} + I_{i1cntcyl}) \\ & + m_3 \gamma_3 (I_{3cnt} + I_{3cntcyl}) + m_{i3} \gamma_{i3} (I_{i3cnt} + I_{i3cntcyl}), \end{aligned} \quad (2.10)$$

where $m_{cnt} = \frac{4}{3} \pi a^3 \rho_{cnt} + \pi a^2 h \rho_{cnt}$, is the mass of CNT and ρ_{cnt} is the density of CNT.

These equations describe the gain in mass density due to collection of atoms of type 1 and 3.

Energy balance equation for spherical CNT tip placed over cylindrical surface

$$\begin{aligned} \frac{d(m_{cnt} C_p T_{cnt})}{d\tau} = & n_{ecnt} \left[\gamma_e \varepsilon_{ec}^s + (1 - \gamma_e) \delta_{ecnt} \left[\varepsilon_{ecnt}^s - \left(\frac{3}{2} k_B \right) T_{cnt} \right] \right] - \left(\frac{3}{2} k_B \right) \\ & \times [n_{1cnt} (\gamma_1 T_n + \delta_{1cnt} (1 - \gamma_1) (T_n - T_{cnt})) + n_{2cnt} \delta_{2cnt} (T_n - T_{cnt}) \\ & + n_{3cnt} (\gamma_3 T_n + \delta_{3cnt} (1 - \gamma_3) (T_n - T_{cnt}))] \\ & + [(I_{i1cnt} + I_{i1cntcyl}) (\varepsilon_{i1cnt}^s + \phi_1) + (I_{i2cnt} + I_{i2cntcyl}) (\varepsilon_{i2cnt}^s + \phi_2) \\ & + (I_{i3cnt} + I_{i3cntcyl}) (\varepsilon_{i3cnt}^s + \phi_3)] \\ & - \left(\frac{3}{2} k_B \right) [(1 - \gamma_{1i}) (I_{i1cnt} + I_{i1cntcyl}) + (I_{i2cnt} + I_{i2cntcyl}) \\ & + (1 - \gamma_{3i}) (I_{i3cnt} + I_{i3cntcyl})] T_{cnt} - (4\pi a^2 + 2\pi a h) \\ & \times \left[\varepsilon \sigma (T_{cnt}^4 - T_a^4) + \left[n_1 \left(\frac{8k_B T_n}{\pi m_1} \right)^{\frac{1}{2}} + n_2 \left(\frac{8k_B T_n}{\pi m_2} \right)^{\frac{1}{2}} + n_3 \left(\frac{8k_B T_n}{\pi m_3} \right)^{\frac{1}{2}} \right] k_B (T_{cnt} - T_n) \right], \end{aligned} \quad (2.11)$$

where C_P is the specific heat of CNT at constant pressure, ε is the emissivity of the material of CNT, σ is the Stefan Boltzmann constant, $\varepsilon_{ijcnt}^s(Q) = \left(\left(\frac{2-Q\alpha_{ji}}{1-Q\alpha_{ji}} \right) - Q\alpha_{ji} \right) k_B T_i$, is the mean energy of j^{th} type ion at the surface of CNT [25], $\varepsilon_{ecnt}^s(Q) = 2k_B T_e$, is the mean energy of electrons at the surface of CNT [25].

First, second and third term of the equation describes the rate of energy transferred to the CNT due to sticking accretion and elastic collision by constituent's species of the plasma. Fourth terms describes the energy per unit volume per unit time carries away from the surface of CNT by the neutral species generated due to recombination of the accreted ions and electrons. Fifth term describes the rate of energy dissipation in the form of radiation and conduction from the CNT to the host gas [26].

Field Enhancement Factor

For the vertical CNT with cylindrical surface, Wang *et al.* [27] obtained an expression for field enhancement factor β of the CNT.

$$\beta = \frac{h}{\rho} + 3.5,$$

where h is the height of the CNT and ρ is the radius of the CNT.

3. Results and Discussions

A theoretical model to study the effect of the hetero-atoms such as B, N, K and Cs on the growth of the CNTs in the complex plasma, is developed in this paper. The mass and energy balance of CNT, charging on CNT, kinetics of electrons, ions and neutral atoms have been incorporated in the present model. Growth of CNTs in complex plasma can occur in different ways like cluster formation, nucleation, coagulation and growth of embryonic nanotubes. We have studied the growth of embryonic nanotubes by condensation in complex plasma because we are willing to investigate the growth process of CNTs in the presence of hetero-atoms. These hetero-atoms act as different dopants on the surface of CNT. Neutral atoms are ionized by the electrons in plasma due to which positive ions and electrons are produced. Various processes are considered in the model like ionization process in which atom or molecule lose or gain electrons and acquire positive or negative charge, respectively, recombination process in which positive ions gain the free electrons or combine with negative ions and form the neutral atoms, sticking of plasma species on the surface of CNT.

To investigate the effect of different doping elements (N, B, K and Cs) on the growth of CNTs, numerical calculations have been carried out. Effect of addition of these dopants on the normalized radius of CNT have been investigated for the fixed number density of CNT (n_{cnt}), electron temperature (T_e), ion temperature (T_i), neutral atom temperature (T_n) and for variable number density of electrons (n_e), number density of ions (n_i), number density of neutral atoms (n_n) because when we change the doping element, number density of ions, electrons and neutral atoms changes. All physical quantities used are taken in CGS units.

Boundary conditions at $\tau = 0$ and all relevant parameters used are, number density of CNT (n_{cnt}) = 10^7 cm^3 , temperature of electron (T_e) = 0.6 eV, temperature of ion (T_i) = 2600 K,

temperature of neutral atom = temperature of CNT ($T_n = T_{cnt}$) = 2000 K, mass of neutral atom = mass of ion of type 1, i.e. Carbon ($m_1 = m_{i1}$) = 12 amu, mass of neutral atom = mass of ion of type 2, i.e. Neon ($m_2 = m_{i2}$) = 20 amu, mass of electron (m_e) = 9.31×10^{-28} g, emissivity of the material of CNT (ϵ) = 0.6, specific heat of CNT at constant pressure (C_P) = 7×10^6 ergs/g K, density of CNT (ρ_{cnt}) = 4.2 g/cm^3 , ionization energy of atom of type 1, i.e. Carbon (ϕ_1) = 11.26 eV, ionization energy of atom of type 2, i.e. Neon (ϕ_2) = 21.5 eV, sticking coefficient of ion and neutral atom of type 1 and 3 ($\gamma_i = \gamma_n$) = 1, initial height of CNT (h_0) = $10 \mu\text{m}$.

Parameters and boundary condition at $\tau = 0$ used for undoped CNT are, number density of ions ($n_{i1} = n_{i2} = n_{i3}$) = 10^{10} cm^{-3} , number density of electrons (n_e) = 10^{10} cm^{-3} , number density of neutral atoms ($n_1 = n_2 = n_3$) = 10^{11} cm^{-3} , coefficient of recombination of electrons with ion of type 1 and 2 ($\alpha_{01} \approx \alpha_{02}$) = $10^{-7} \text{ cm}^3/\text{s}$, initial radius of CNT (a_0) = 1.1 nm.

Parameters and boundary condition at $\tau = 0$ used for Boron doped CNT are, number density of ions ($n_{i1} = n_{i2} = n_{i3}$) = 10^{10} cm^{-3} , number density of electrons (n_e) = 10^{10} cm^{-3} , number density of neutral atoms ($n_1 = n_2 = n_3$) = 10^{12} cm^{-3} , coefficient of recombination of electrons with ion of type 1 and 2 ($\alpha_{01} \approx \alpha_{02}$) = $1.08 \times 10^{-7} \text{ cm}^3/\text{s}$, initial radius of CNT (a_0) = 1.43 nm, ionization energy of atom of type 3, i.e., Boron (ϕ_3) = 8.3 eV, mass of neutral atom = mass of ion of type 3 ($m_3 = m_{i3}$) = 10.8 amu.

Parameters and boundary condition at $\tau = 0$ used for Potassium doped CNT are, number density of ions ($n_{i1} = n_{i2} = n_{i3}$) = 10^{12} cm^{-3} , number density of electrons (n_e) = 10^{12} cm^{-3} , number density of neutral atoms ($n_1 = n_2 = n_3$) = 10^{11} cm^{-3} , coefficient of recombination of electrons with ion of type 1 and 2 ($\alpha_{01} \approx \alpha_{02}$) = $1.21 \times 10^{-7} \text{ cm}^3/\text{s}$, initial radius of CNT (a_0) = 0.91 nm, ionization energy of atom of type 3, i.e., Potassium (ϕ_3) = 4.3 eV, mass of atom = mass of ion of type 3 ($m_3 = m_{i3}$) = 39.08 amu.

Parameters and boundary condition at $\tau = 0$ used for Cesium doped CNT are, number density of ions ($n_{i1} = n_{i2} = n_{i3}$) = 10^{11} cm^{-3} , number density of electrons (n_e) = 10^{11} cm^{-3} , number density of neutral atoms ($n_1 = n_2 = n_3$) = 10^{10} cm^{-3} , coefficient of recombination of electrons with ion of type 1 and 2 ($\alpha_{01} \approx \alpha_{02}$) = $1.31 \times 10^{-7} \text{ cm}^3/\text{s}$, initial radius of CNT (a_0) = 0.84 nm, ionization energy of atom of type 3, i.e., Cesium (ϕ_3) = 3.8 eV, mass of atom = mass of ion of type 3 ($m_3 = m_{i3}$) = 132.9 amu.

Parameters and boundary condition at $\tau = 0$ used for Nitrogen doped CNT are, number density of ions ($n_{i1} = n_{i2} = n_{i3}$) = 10^{11} cm^{-3} , number density of electrons (n_e) = 10^{11} cm^{-3} , Number density of neutral atoms ($n_1 = n_2 = n_3$) = 10^9 cm^{-3} , coefficient of recombination of electrons with ion of type 1 and 2 ($\alpha_{01} \approx \alpha_{02}$) = $1.54 \times 10^{-7} \text{ cm}^3/\text{s}$, initial radius of CNT (a_0) = 0.73 nm, ionization energy of atom of type 3, i.e., Nitrogen (ϕ_3) = 14.5 eV, mass of atom = mass of ion of type 3 ($m_3 = m_{i3}$) = 14 amu.

Figure 1(a) represents the growth of undoped CNT (Spherical tip placed over cylindrical surface) with respect to time. From the graph, we can interpret that normalized radius of the undoped CNT increases with time and get saturated after some time. This is because accretion of neutral atoms on the surface of CNT increases with time. The value of sticking coefficient of atom of type 1 is the important parameter for the growth of CNTs, as value of sticking coefficient increases, saturation region is achieved faster. When number of neutral atoms on the surface

of CNT increases, negative charge on the CNT decreases, which stops the further accretion of neutral atoms on the surface of the CNT and radius of the CNT attains the saturated value.

Figure 1(b) illustrates the variation of the normalized radius of the Boron doped carbon nanotube. Growth pattern is same as of undoped CNT but radius of the boron doped CNT is greater than the radius of the undoped CNT. Boron consumes electrons to form the covalent bonding with carbon to attain stability, thereby reducing the number density of electrons which reduces the ionization of neutral atoms and accretion of neutral atoms on the surface of CNT increases, hence radius of the CNT increases.

Figure 1(c) and Figure 1(d) show the variation of normalized radius of CNT when doped with alkali metals like Potassium (K) and Cesium (Cs), respectively. Growth pattern is same as of undoped CNT but radius of alkali metal doped CNT is less than the undoped CNT. Being a metal, Potassium and Cesium release electrons to form the stable bond with carbon. This increases the number density of electrons, thereby ionization of neutral atoms increases hence radius of the CNT decreases. But the radius of the Cesium doped CNT is less than the radius of Potassium doped CNT this is because, free electrons in Cesium are loosely bound than the Potassium therefore ionization of neutral atoms is more in Cesium doped CNT than the Potassium doped CNT hence accretion of neutral atoms in the case of Cesium doped CNT is less due to which radius is less than the Potassium doped CNT.

Figure 1(e) shows the time evolution of the normalized radius of the Nitrogen doped CNT. From all five figs. we can see that radius of the Nitrogen doped CNT is least among all doped CNTs. Nitrogen is penta valent element i.e. contains five electrons in outer most shell, to attain the stability it requires three more electrons. Therefore ionization of neutral atoms is maximum in the case of Nitrogen doped CNT and accretion of neutral atoms on the surface of CNT is least and radius is minimum among all doped CNTs.

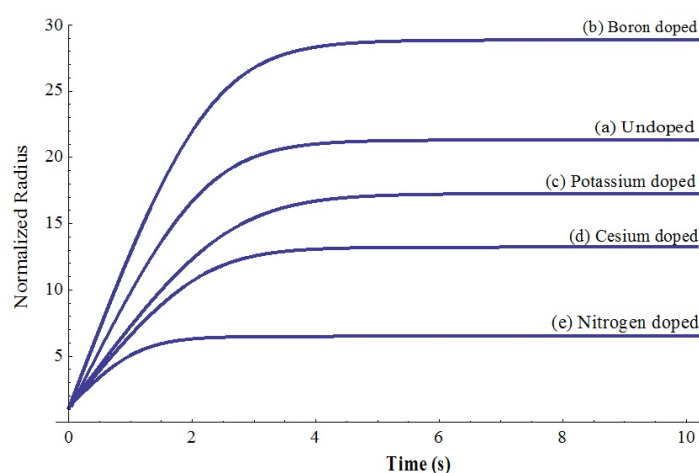


Figure 1. Illustrates the growth of normalized radius of spherical CNT tip placed over cylindrical surface for (a) boron doped CNT, (b) undoped CNT, (c) Potassium doped CNT, (d) Cesium doped CNT and (e) nitrogen doped CNT.

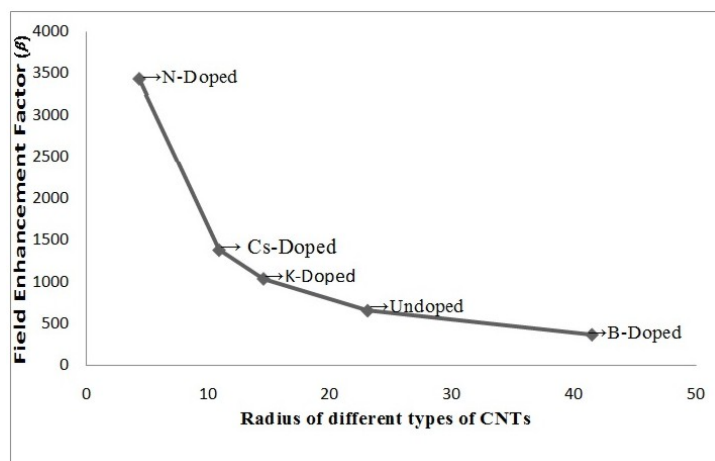


Figure 2. Shows the dependence of the field enhancement factor on the radius of different types of CNTs, i.e., undoped CNT, Boron doped CNT, Potassium doped CNT, Cesium doped CNT and Nitrogen doped CNT.

Figure 2 shows the variation of the field enhancement factor with respect to the radius of the CNT at constant height. From the results obtained, field enhancement factor for the different CNTs have been roughly estimated at the constant height, we have calculated the radius of all different types of CNTs and we get 23.1 nm for undoped CNT, 41.47 nm for boron doped CNT, 14.56 nm for potassium doped CNT, 10.92 nm for cesium doped CNT and 4.38 for nitrogen doped CNT, height of the CNT is considered to be 15 μm and field enhancement factor are obtained as 652.85, 365.20, 1033.71, 1377.12 and 3428.15 for undoped, boron doped, potassium doped, cesium doped and nitrogen doped CNTs, respectively. The graph between field enhancement factor and radius of the different CNTs shows that as radius (a) of the CNT decreases, field enhancement factor (β) of the CNT increases i.e. Nitrogen doped CNT has highest field emission factor and boron doped CNT has lowest field emission factor. The similar plot has been obtained experimentally by Xu *et al.* [1].

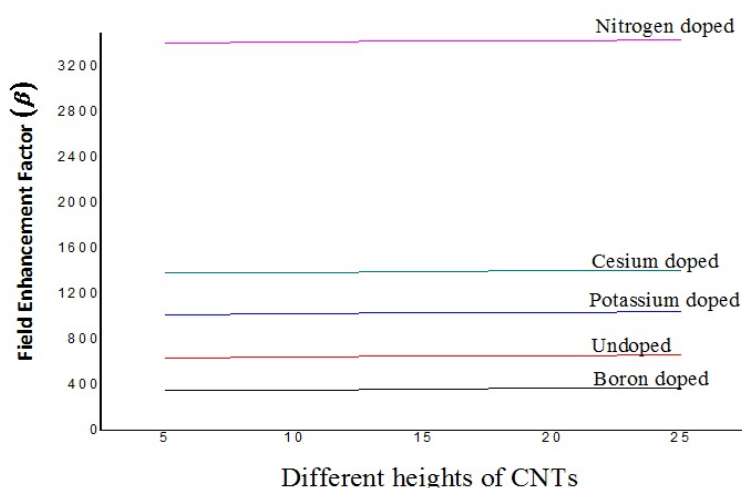


Figure 3. Displays the variation of the field enhancement factor with respect to the different heights of CNT for undoped CNT, Boron doped CNT, Potassium doped CNT, Cesium doped CNT and Nitrogen doped CNT.

Figure 3 shows the effect of height on the field enhancement factor of different CNTs. Radius and field emission properties of CNTs have been calculated corresponding to the different heights of CNTs. We found that the height of the CNT hardly effect the field enhancement factor of the CNT. Results obtained have also been experimentally verified by Xu *et al.* [1].

Similar results have been observed experimentally by Padya *et al.* [28], Srivastava *et al.* [8], Chan *et al.* [29], Zhang *et al.* [10], Ha and Lee [30] and Wadhawan *et al.* [14]. Therefore, doping of CNT tip with nitrogen atom can lead to enhance field emission properties. This has multiple applicative utilizations in the field of microelectronics, nanoscience and Technology.

4. Conclusion

A theoretical model has been developed for calculating the radius of spherical CNT tip placed over the cylindrical surface with different doping elements. The effect of different dopants has been studied with the help of an analytical model. The charging of CNT, charge neutrality, growth of electron density, neutral atom and positive ions density and energy balance of CNT with different doping elements are included in the model. It can be seen that decrease in the radius of the CNT is larger when CNT is doped with nitrogen. We conclude that radius of the CNTs has enormous effect of the field emission properties of the CNT whereas height of the CNTs does not play an important role to influence the field emission properties of the CNTs.

Competing Interests

The authors declare that they have no competing interests.

Authors' Contributions

All the authors contributed equally and significantly in writing this article. All the authors read and approved the final manuscript.

References

- [1] Z. Xu, X.D. Bai and E.G. Wang, *Appl. Phys. Lett.* **88** (2006), 133107.
- [2] J.M. Bonard, J.P. Salvetat, T. Stockli, W.A. De Heer, L. Forro and A. Chatelain, *Appl. Phys. Lett.* **73** (1998), 918.
- [3] K.W. Wong, X.T. Zhou, F.C.K. Au, H.L. Lai, C.S. Lee and S.T. Lee, *Appl. Phys. Lett.* **75** (1999), 2918.
- [4] J.M. Bonard, J.P. Salvetat, T. Stockli, L. Forro and A. Chatelain, *Appl. Phys. A* **69** (1999), 245.
- [5] K.A. Dean and B.R. Chalamala, *Appl. Phys. Lett.* **76** (1999), 375.
- [6] S.K. Srivastava, V.D. Vankar and V. Kumar, *Nanoscale Res. Lett.* **3** (2008), 25.
- [7] A.A. Koos, F. Dillon, E.A. Obraztsova, A. Crossley and N. Grobert, *Carbon* **48** (2010), 3033.
- [8] S.K. Srivastava, V.D. Vankar, D.V.S. Rao and V. Kumar, *Thin Solid Films* **515** (2006), 1851.
- [9] D.H. Lee, J.A. Lee, D.S. Choi, W.J. Lee and S.O. Kim, *J. Phys. Chem. C* **114** (2010), 21184.
- [10] G. Zhang, W. Duan and B. Gu, *Appl. Phys. Lett.* **80** (2002), 2589.

- [11] A.S. Claye, J.E. Fischer, C.B. Huffman, A.G. Rinzler and R.E. Smalley, *J. Electrochem. Soc.* **147** (2000), 2845.
- [12] W. Zhou, J. Vavro, N.M. Nemes and J.E. Fischer, *Phys. Rev. B* **71** (2005), 205423.
- [13] M. Salvato, M. Lucci, I. Ottaviani and M. Cirillo, *Phys. Rev. B* **84** (2011), 233406.
- [14] A. Wadhawan, R.E. Stallcup and J.M. Perez, *Appl. Phys. Lett.* **78** (2001), 108.
- [15] S.Y. Choi, Y. Kanng, K.I. Cho, K.S. Choi and D. Kim, *J. Korean Phys. Soc.* **39** (2001), 193.
- [16] Y.Y. Wang, S. Gupta, J.M. Garguilo, Z.J. Liu, L.C. Qin and R.J. Nemanich, *Diamond Relat. Mater.* **14** (2005), 714.
- [17] J.M. Bonard, J.P. Salvetat, T. Stockli and W.A. De Heer, *Appl. Phys. Lett.* **73** (1998), 918.
- [18] I. Levchenko, K. Ostrikov, A.E. Rider, E. Tam, S.V. Vladimirov and S. Xu, *Phys. Plasmas* **14** (2007), 0632502.
- [19] M. Keidar, I. Levenchko, T. Arbel, M. Alexander, A.M. Waas and K.K. Ostrikov, *J. Appl. Phys.* **103** (2008), 094318.
- [20] B.B. Wang, Q.J. Cheng, X. Chen and K. Ostrikov, *J. Alloys Compd.* **509** (2011), 9329.
- [21] A. Tewari and S.C. Sharma, *Phys. Plasmas* **21** (2011), 063512.
- [22] M.S. Sodha, S.K. Mishra and S. Srivastava, *J. Appl. Phys.* **107** (2010), 103307.
- [23] M.S. Sodha, S.K. Mishra and S. Misra, *Phys. Plasmas* **16** (2009), 123701.
- [24] A. Tewari and S.C. Sharma, *J. Plasma Phys.* **79** (2013), 939.
- [25] M.S. Sodha and S. Guha, in *Physics of Colloidal Plasmas*, edited by A. Simon and W.B. Thomson (John Wiley & Sons, New York, 1971), p. 219.
- [26] M. Rosenberg, D.A. Mendis and D.P. Sheehan, *IEEE Trans. Plasma Sci.* **27** (1999), 239.
- [27] X.Q. Wang, M. Wang, P.M. He and Y.B. Xu, *J. Appl. Phys.* **96** (2004), 6752.
- [28] B. Padya, D. Kalita, P.K. Jain, G. Padmanabham, M. Ravi and K.S. Bhat, *Appl. Nanosci.* **2** (2012), 253.
- [29] L.H. Chan, K.H. Hong, D.Q. Xiao, W.J. Hsieh, S.H. Lai, H.C. Shih, T.C. Lin, F.S. Shieu, K.J. Chen and H.C. Cheng, *Appl. Phys. Lett.* **82** (2003), 4334.
- [30] B. Ha and C.J. Lee, *Appl. Phys. Lett.* **90** (2007), 023108.